
SyntheOcc: Synthesize Geometric-Controlled Street View Images through 3D Semantic MPIs

Anonymous Author(s)

Affiliation

Address

email

Abstract

1 The advancement of autonomous driving is increasingly reliant on high-quality
2 annotated datasets, especially in the task of 3D occupancy prediction, where the
3 occupancy labels require dense 3D annotation with significant human effort. In
4 this paper, we propose **SyntheOcc**, which denotes a diffusion model that Synthesize
5 photorealistic and geometric-controlled images by conditioning Occupancy labels
6 in driving scenarios. This yields an unlimited amount of diverse, annotated, and
7 controllable datasets for applications like training perception models and simulation.
8 SyntheOcc addresses the critical challenge of how to efficiently encode
9 3D geometric information as conditional input to a 2D diffusion model. Our approach
10 innovatively incorporates 3D semantic multi-plane images (MPIs) to provide
11 comprehensive and spatially aligned 3D scene descriptions for conditioning.
12 As a result, SyntheOcc can generate photorealistic multi-view images and videos
13 that faithfully align with the given geometric labels (semantics in 3D voxel space).
14 Extensive qualitative and quantitative evaluations of SyntheOcc on the nuScenes
15 dataset prove its effectiveness in generating controllable occupancy datasets that
16 serve as an effective data augmentation to perception models.

17 1 Introduction

18 With the rapid development of generative models, they have shown realistic image synthesis and
19 diverse controllability. This progress has opened up new avenues for dataset generation in autonomous
20 driving [5, 12, 23, 30]. The task of dataset generation is usually modeled as controllable image
21 generation, where the ground truth (*e.g.* 3D Box) is employed to control the generation of new datasets
22 in downstream tasks (*e.g.* 3D detection). This approach helps to mitigate the data collection and
23 annotation effort as it can generate labeled data for free. However, a novel task of vital importance,
24 occupancy prediction [24, 27], poses new challenges for dataset generation compared with 3D
25 detection. It requires finer and more nuanced geometry controllability, which refers to use the
26 occupancy state and semantics of voxels in the whole 3D space to control the image generation.
27 We argue that solving this problem not only allows us to synthesize occupancy datasets, but also
28 empowers valuable applications such as editing geometry to generate rare data for corner case
29 evaluation, as shown in Fig. 1. In the following, we first illustrate why prior work struggles to achieve
30 the above objective, and then demonstrate how we address these challenges.

31 In the area of diffusion models, several representative works have displayed high-quality image
32 synthesis; however, they are constrained by limited 3D controllability: they are incapable of editing 3D
33 voxels for precise control. For example, BEVGen [23] generates street view images by conditioning
34 BEV layouts using diffusion models. MagicDrive [5] extend BEVGen and additionally converts the
35 3D box parameters into text embedding through Fourier mapping that is similar to NeRF [19], and
36 uses cross-attention to learn conditional generation. Although these methods achieve satisfactory
37 results in image generation, their 3D controllability is inherently limited. These approaches are

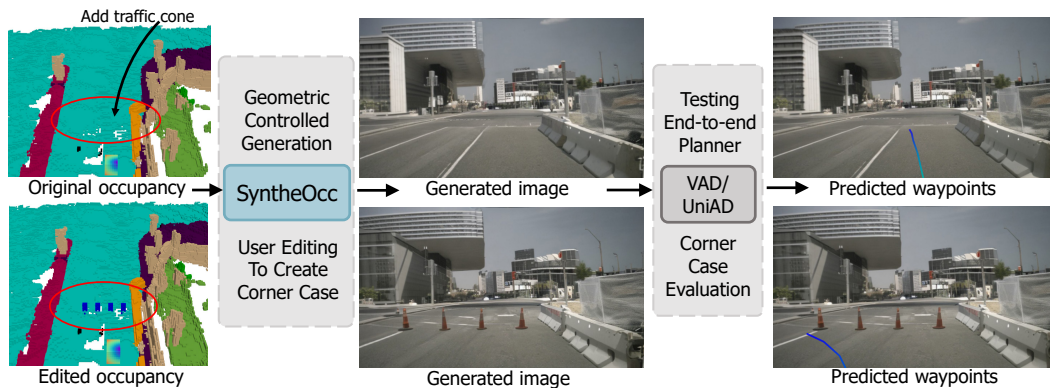


Figure 1: A showcase of application of **SytheOcc**. We enable geometric-controlled generation that conveys the user editing in 3D voxel space to generate realistic street view images. In this case, we create a rare scene that traffic cones block the way. This advancement facilitates the evaluation of autonomous systems, such as the end-to-end planner VAD [9], in simulated corner case scenes.

38 restricted to manipulating the scene in types of 3D boxes and BEV layouts, and hardly adapt to finer
 39 geometry control such as editing the shape of objects and scenes. Meanwhile, they usually convert
 40 conditional input into 1D embedding that aligns with prompt embedding, which is less effective in
 41 3D-aware generation due to lack of spatial alignment with the generated images. This limitation
 42 hinders their utility in downstream applications, such as occupancy prediction and editing scene
 43 geometry to create long-tailed scenes, where granular volumetric control is paramount in both tasks.

44 ControlNet [41] and GLIGEN [14] is another type of prominent method in the field of controllable
 45 image generation. These approaches exhibit several desirable attributes in terms of controllability.
 46 They leverage conditional images such as semantic masks for control, thereby offering a unified
 47 framework to manipulate both foreground and background. However, despite its precise spatial
 48 control, ControlNet does not align with our specific requirements. Their conditions of pixel-level
 49 images differ fundamentally from what we require in 3D contexts. Our experimental results also find
 50 that ControlNet struggles to handle overlapping objects with varying depths (see Fig. 6 (a)), as it only
 51 utilizes an ambiguous 2D semantic map as conditional input. As a result, it is non-trivial to extend
 52 the ControlNet framework and convey their desirable attributes for 3D conditioning.

53 To address the above challenges, we propose an innovative representation, 3D semantic multi-plane
 54 images (MPIs), which contribute to image generation with finer geometric control. In detail, we
 55 employ multi-plane images [43] to represent the occupancy, where each plane represents a slice of
 56 semantic label at a specific depth. Our 3D semantic MPIs not only preserve accurate and authentic 3D
 57 information, but also keep pixel-wise alignment with the generated images. We additionally introduce
 58 the MPI encoder to encode features, and the reweighing methods to ease the training with long-tailed
 59 cases. As a collection, our framework enables 3D geometry and semantic control for image generation
 60 and further facilitates corner case evaluation as depicted in Fig. 1. Finally, experimental results
 61 demonstrate that our synthetic data achieve better recognizability, and are effective in improving the
 62 perception model on occupancy prediction. In summary, our contributions include:

- 63 • We present **SytheOcc**, a novel image generation framework to attain finer and precise 3D
 64 geometric control, thereby unlocking a spectrum of applications such as 3D editing, dataset
 65 generation, and long-tailed scene generation.
- 66 • Incorporating the proposed 3D semantic MPI, MPI encoder, and reweighing strategy, we
 67 deliver a substantial advancement in image quality and recognizability over prior works.
- 68 • Our extensive experimental results demonstrate that our synthetic data yields an effective
 69 data augmentation in the realm of 3D occupancy prediction.

70 2 Related Work

71 2.1 3D Occupancy Prediction

72 The task of 3D occupancy prediction aims to predict the occupancy status of each voxel in 3D space,
 73 as well as its semantic label if occupied. Compared with previous perception methods like 3D object

74 detection, occupancy prediction offers a more detailed and nuanced understanding of the environment,
75 as it provides finer geometric details, is capable of handling general, out-of-vocabulary objects, and
76 finally, enriches the planning stack with comprehensive 3D information. Early methods exploited
77 LiDAR as inputs to complete the 3D occupancy of the entire 3D scene [18, 33]. Recent methods
78 began to explore the more challenging vision-based 3D occupancy prediction [24, 25, 27, 29]. By
79 predicting the geometric and semantic properties of both dynamic and static elements, 3D occupancy
80 prediction offers a more comprehensive understanding of the surrounding environment.

81 2.2 Diffusion-based Image Generation

82 Recent advancements in diffusion models (DMs) have achieved remarkable progress in image
83 generation. In particular, Stable Diffusion (SD) [21] employs DMs within the latent space of
84 autoencoders, striking a balance between computational efficiency and high image quality. Beyond
85 text control, there is also the introduction of additional control signals. A noteworthy work is
86 ControlNet [41], which incorporates a trainable copy of the SD encoder to extract the feature of
87 conditional images and adds it to the UNet feature. It significantly enhances the controllability and
88 unlocking pathways for advanced applications. We refer readers to recent survey [35] for more details.

89 2.3 Image Generation in Autonomous Driving

90 As training neural networks relies heavily on labeled data, numerous studies are delving into dataset
91 generation to boost training. Lift3D [12] designs generative NeRF to synthesize labeled datasets
92 for 3D detection for the first time. Several other works employ BEV layouts to synthesize image
93 data, proving beneficial for perception models. For example, BEVGen [23] conditions BEV layouts
94 to generate multi-view street images, while BEVControl [34] separately generates foregrounds and
95 backgrounds from BEV layouts. MagicDrive [5] generates images with 3D geometry controls by
96 independently encoding objects and maps through a text encoder or map encoder. Compared with
97 MagicDrive, our geometry control is characterized by a more detailed and lossless representation of
98 3D scenes for control, which poses significant challenges than projected layout or box embedding.

99 Recently, DriveDreamer [26], DrivingDiffusion [13], Drive-WM [28] and Panacea [30] use a Con-
100 trolNet framework, which involves projecting bounding boxes and road maps onto 2D FoV images as
101 a conditioning input. This approach has proven to be effective for geometric control. However, it is
102 limited in that it only achieves alignment at the 2D-pixel level. Consequently, this method falls short
103 in capturing the depth hierarchy and fails to account for the occlusion relationships present in the 3D
104 real world. Besides, adding a depth channel like Panacea [30] may address the limitations of depth
105 order, but it discards the occluded part and only contains partial observation. UrbanGiraffe [37] train
106 a generative NeRF to perform image generation. WoVoGen [17] creates a 4D world volume feature
107 using occupancy to guide the generation, but seems to rely on object mask guidance.

108 As described above, most of the prior work is restricted by only modeling a projected primitive of 3D
109 boxes and road maps as conditions. They suffer from ill-posed un-projection ambiguity. In contrast,
110 we model 3D occupancy labels as conditions, as they provide finer geometric details and semantic
111 information. However, designing an input representation of 3D occupancy labels into a 2D diffusion
112 model is challenging. In this paper, we propose a novel representation: 3D semantic Multi-Plane
113 Images (MPIs) as conditional inputs, which not only provide spatial alignment that improves visual
114 consistency, but also encode comprehensive 3D geometric information including occluded parts.

115 3 Method

116 **Overview** The overview of our method is depicted in Fig. 2. Built upon the SD pipeline, we
117 aim to perform geometry-controlled image generation by conditioning on 3D geometry labels with
118 semantics (occupancy labels). One requirement is that the images should faithfully align with the
119 given label. This task is more challenging than conditioned on 3D box due to the sparse and irregular
120 nature of occupancy. We first discuss how to efficiently represent occupancy in Sec. 3.2, followed
121 by our designed MPI encoder to enhance generation quality in Sec. 3.3, and reweighing strategy to
122 handle the long-tailed depth and category in Sec. 3.5.

123 3.1 Representation of Condition: Local Control Aligns Better than Global Control

124 One of the key challenges is how to represent our conditional occupancy input. A straightforward
125 method [3, 5] is to convert the 3D occupancy voxel to 1D global embedding that is similar to text
126 embedding, and then use cross-attention to learn controllable generation. However, these global
127 methods can be less effective when dealing with dense or irregular data due to the following reasons:

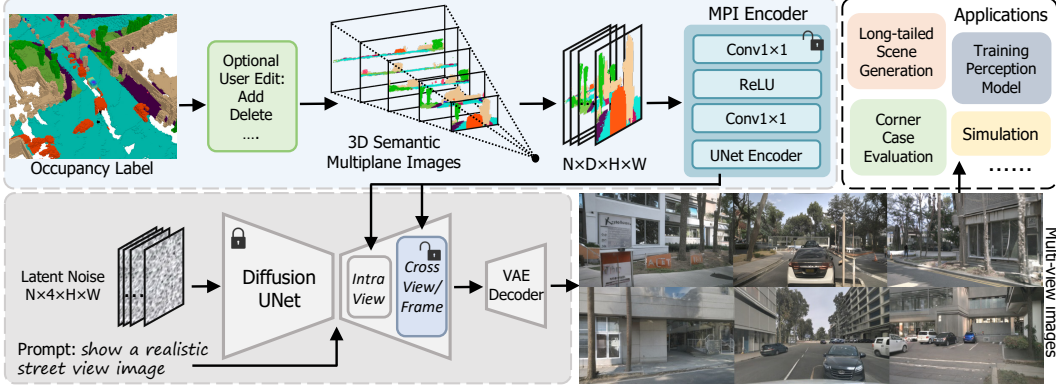


Figure 2: The overall architecture of **SytheOcc**. We achieve 3D geometric control in image generation by utilizing our proposed 3D semantic multiplane images to encode scene occupancy. In our framework, we can edit the occupied state and semantics of every voxel in 3D space to control the image generation, thereby opening up a wide spectrum of applications as shown in the top right.

128 (i) They perform controllable generation through hard encoding the spatial relationship between 1D
 129 global embedding and 2D UNet features. (ii) Ignore the underlying geometry alignment between the
 130 conditional input and the generated image. In contrast, local methods like ControlNet, directly add
 131 spatial features to the UNet features, providing 2D local control with pixel-level spatial alignment.
 132 They are better than the global method (see Tab. 1), but suffer from 3D ambiguity (see Fig. 6 (a)).
 133 Consequently, this comparison motivates us to seek a more compact and efficient manner to encode
 134 and condition our 3D occupancy labels.

135 3.2 Represent Occupancy as 3D Semantic Multiplane Images

136 It is non-trivial to design a 3D representation for conditioning. To efficiently store both the semantic
 137 and geometric information of the irregular occupancy input, we propose to use multiplane images
 138 (MPIs) [43] as representation. An MPI is composed of a series of fronto-parallel RGBA layers within
 139 the frustum of the source camera with a specific viewpoint. These planes are arranged at varying
 140 depths, from d_{min} to d_{max} , starting from the nearest to the farthest. Each layer of these images
 141 contains both an RGB image and an alpha map, which collectively capture the visual and geometric
 142 details of the scene at the respective depth. In our work, instead of storing RGB value and alpha map
 143 in the original MPI, we store our 3D semantic labels. Each layer of MPI represents the semantic
 144 index at the corresponding depth. We display the colored MPI in the top row of Fig. 2 for visual
 145 clarity, but we actually use the integer index for learning. We obtain our 3D semantic MPI by:

$$P_l = (u \times d_l, v \times d_l, d_l)^T, \quad d_l = d_{min} + (d_{max} - d_{min}) \times l/D, \quad (1)$$

$$\text{MPI}_{n,l} = \text{Interpolate}(\text{Occupancy}, \mathbf{T}_n \cdot \mathbf{K}_n^{-1} \cdot P_l), \quad (2)$$

$$\text{MPI} = \text{Concatenate}(\text{MPI}_{i,j}), \quad i \in (0, N), \quad j \in (0, D), \quad (3)$$

146 where (u, v) is a pixel coordinate in image space, d_l is depth value of the l^{th} layer, n denotes the n^{th}
 147 camera view. This equation implies we first back project points P in camera frustum space (u, v, d)
 148 to Euclid space (x, y, z) by multiplying inverse intrinsic \mathbf{K}^{-1} . Then we use transformation matrix \mathbf{T}
 149 to map points from camera coordinates to occupancy coordinates. We then use the point coordinates
 150 to interpolate the nearest semantic index from the dense occupancy voxel to form a slice of MPI.
 151 Finally, we concatenate all slices to form $\text{MPI} \in \mathbb{R}^{N \times D \times H \times W}$, where D is the number of layers that
 152 is set at 256, N is the number of camera views in the case of batch size = 1.

153 By representing occupancy as 3D semantic MPI, every pixel in MPI contains geometry and semantic
 154 information with implicit depth, seamlessly integrating occluded elements, and ensuring a precise
 155 spatial alignment with the generated images.

156 3.3 3D Semantic MPI Encoder

157 To enable local control with spatially aligned conditions, we develop a simple but effective MPI
 158 encoder that aligns the 3D multi-plane feature to the latent space of the diffusion model. The
 159 purpose of the MPI encoder is to obtain features from multi-plane images to perform 3D-aware



Figure 3: Visualizations of geometric controlled generation. **Top row**: Fusion of 3D semantic MPI. **Bottom row**: our generation concatenated from neighboring views.

160 image synthesis. Unlike the original ControlNet which downsampling conditional input through 3×3
 161 convolutions with padding, we design a 1×1 convolutional encoder without downsampling to encode
 162 features. In detail, the 3D multiplane features which have the sample resolution with latent features,
 163 are transformed by a 1×1 convolution layer and ReLU activation [1] in the MPI encoder.

164 After obtaining the multi-scale feature after the MPI encoder, we add the feature to the decoder of
 165 diffusion UNet to provide spatial features. Experimental results in Tab. 3 will show that our 1×1 conv
 166 in MPI encoder is more effective than 3×3 conv, as the 1×1 conv with receptive field = 1 provides a
 167 spatial align feature to the latent feature in the diffusion UNet. In contrast, 3×3 conv is conducted
 168 in a camera frustum space rather than Euclid space, making an imprecise correspondence between
 169 3D multiplane features and 2D image features. Moreover, using 3×3 conv to process 3D semantic
 170 MPI will introduce a large computational burden as the channel number increases from 3 channels of
 171 RGB to 256 planes. We display our 3D geometry and semantic control property in Fig. 3.

172 In summary, we chose MPIs as the representation because they (i) Incorporate lossless 3D information,
 173 including scene geometry rather than 2.5D depth. (ii) Provide spatially aligned conditional features
 174 that naturally extend the ControlNet framework from image level to 3D level. (iii) Capable of
 175 representing geometry and semantics including occluded elements.

176 3.4 Cross-View and Cross-Frame Attention

177 The sensor arrangement in a self-driving car usually requires a full surround view of cameras to capture
 178 the entire 360-degree environment. To effectively simulate the multi-view and subsequent multi-frame
 179 generation, zero-initialized [41] cross-view and cross-frame attention are integrated into the diffusion
 180 model to maintain consistency between views and frames. Following prior work [5, 28, 30, 31],
 181 each cross-view attention allows the target view to access information from its neighboring left and
 182 right views, thus training cross-view attention using multi-view consistent images will enforce it to
 183 generate the same instance in the overlapping region of multi-view cameras.

$$\text{Attention}(Q, K, V) = \text{softmax}\left(\frac{QK^T}{\sqrt{d}}\right) \cdot V, \quad (4)$$

$$h_{out} = h_{in} + \sum_{i \in \{l, r\}} \text{Attention}(Q_{in}, K_i, V_i), \quad (5)$$

184 where l , and r is the camera view of left and right. Q_{in} and h_{in} denotes the query and the hidden
 185 state of input view. Similarly, we add cross-frame attention that attend previous frame and future
 186 frame to enable video generation. In this case, we use the same formulation while $i \in \{f, h\}$, where
 187 f and h is the camera view of future and history frames.

188 3.5 Importance Reweighting

189 To deal with the extreme imbalance problem between
 190 foreground, background, and object categories, and
 191 also to ease the training, we propose three types of
 192 reweighting methods to improve the generation quality
 193 of foreground objects.

194 **Progressive Foreground Enhancement** To miti-
 195 gate the complexity of the learning task, we propose a
 196 progressive reweighting method that incrementally en-
 197 hances the loss associated with the foreground regions
 198 (based on semantic class) as the training progresses.
 199 The detailed formulation is:

$$w(x, m, n) = \frac{(m-1)}{2} \cdot \left(1 + \cos\left(\frac{x}{n} \cdot \pi + \pi\right)\right) + 1, \quad (6)$$

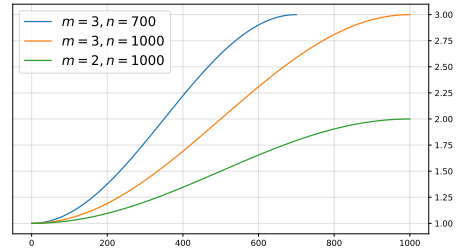


Figure 4: Visualizations of the reweighting function in Eq. 6.

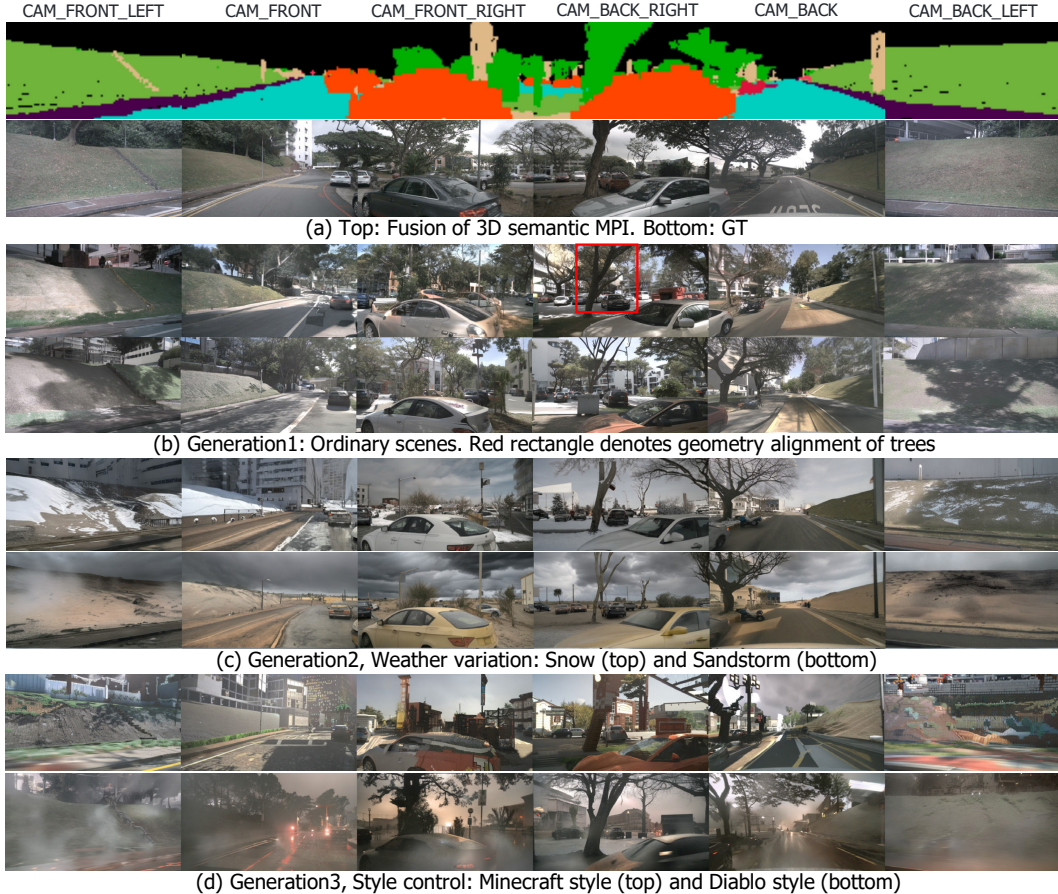


Figure 5: Visualizations of generated multi-view images. The generation conditions (occupancy labels) are from nuScenes validation set. We highlight that (i) Geometry alignment of trees in red rectangle in (b). (ii) Use text prompt to control high-level appearance in (c,d).

200 where x is the current training step, m is the maximum value of weights that set at 2, and n is the
 201 total training steps. This approach is engineered to facilitate a learning trajectory that progresses
 202 from simplicity to complexity, thereby aiding in the convergence of the model. This curve can be
 203 interpreted as a cosine annealing but inverted to amplify the importance of the foreground region.

204 **Depth-aware Foreground Reweighting** In the meantime, we acknowledge the learning difficulty
 205 in different depth places in 3D scenes. Following GeoDiffusion [3], we perform depth reweighting to
 206 foreground objects by adaptively assigning higher weights to farther foreground areas. This enables
 207 the model to focus more thoroughly on hard examples with depth-aware importance reweighting.
 208 Instead of using their exponential function to increase weights, we use our designed cosine function
 209 Eq. 6 for stability. Here x is the input depth value, and n is the maximum depth that set at 50.

210 **CBGS Sampling** To deal with the class imbalance problem in driving scenarios, where cer-
 211 tain object categories appear infrequently, we employ the Class-Balanced Grouping and Sampling
 212 (CBGS) [44] to better handle the long-tailed classes. CBGS addresses the challenge of class imbal-
 213 ance by grouping and re-sampling training data to ensure each group has a balanced distribution of
 214 sample frequency across different object categories. This method reduces the bias towards more
 215 frequent classes and enables better generalization to rare scenarios.

216 3.6 Model Training

217 To ease the training of the MPI encoder and added attention module, we use a two stage training
 218 pipeline. We first train MPI encoder and cross-view attention in a multi-view image generation setting.
 219 Then we train cross-frame attention and freeze other components in a video generation setting.

Method	Train	Val	mIoU	barrier	bicycle	bus	car	cons. veh.	moto.	pedes.	traf. cone	trailer	truck	drive. suf.	other flat	sidewalk	terrain	manmade	vegetation
				■	■	■	■	■	■	■	■	■	■	■	■	■	■	■	■
Oracle (FB-Occ [15])	Real	Real	39.3	45.4	28.2	44.1	49.4	25.9	28.8	28.0	27.7	32.4	37.3	80.4	42.2	49.9	55.2	42.0	37.7
SytheOcc-Aug	Real+Gen	Real	40.3	45.4	27.2	46.6	49.5	26.4	27.8	28.4	29.4	34.0	37.2	81.3	46.0	52.4	56.5	43.3	38.9
MagicDrive	Real	Gen	13.4	0.7	0.0	11.8	32.4	0.0	6.6	2.8	0.3	2.6	19.6	60.1	12.1	26.2	23.4	15.5	12.8
ControlNet	Real	Gen	17.3	17.7	0.2	13.6	21.0	0.6	0.8	8.6	10.4	6.9	11.9	67.4	18.8	36.4	36.9	20.8	22.4
ControlNet+depth	Real	Gen	17.5	19.3	0.3	14.0	23.7	1.0	0.6	9.2	9.2	5.7	12.1	68.8	19.2	36.0	35.3	19.8	22.8
SytheOcc-Gen	Real	Gen	25.5	32.6	13.8	27.7	33.4	7.5	6.5	15.7	16.5	16.5	25.6	74.3	24.5	39.4	40.5	28.6	28.8

Table 1: Downstream evaluation on the **nuScenes-Occupancy** validation set. Based on the used train and val data, two types of settings are reported. The first is to use generated training set to augment the real training set, and evaluate on the real validation set, denoted as Aug. The second is to use pretrained models trained on the real training datasets to test on the generated validation set, denoted as Gen.

220 **Objective Function** Our final objective function can be formulated as a standard denoising
221 objective with reweighing:

$$\mathcal{L} = \mathbb{E}_{\mathcal{E}(x), \epsilon, t} \|\epsilon - \epsilon_{\theta}(z_t, t, \tau_{\theta}(y))\|^2 \odot w, \quad (7)$$

222 where w is the multiplication of progressive reweighing and depth-aware reweighing.

223 4 Experiments

224 4.1 Dataset and Setups

225 We conduct our experiments on the nuScenes dataset [2], which is collected using 6 surrounded-view
226 cameras that cover the full 360° field of view around the ego-vehicle. It contains 700 scenes for
227 training and 150 scenes for validation. We resize the original image from 1600 × 900 to 800 × 448 for
228 training. In our work, we use the occupancy label with a resolution of 0.2m from OpenOccupancy [27]
229 as condition input, while the benchmark of occupancy prediction uses a resolution of 0.4m from
230 Occ3D [24] dataset for its popularity.

231 **Networks** We use Stable Diffusion [21] v2.1 checkpoint as initialization and only train occupancy
232 encoder, cross-view attention. We additionally add cross-frame attention if in video experiments. We
233 adopt FB-Occ [15] as the target model for occupancy prediction for its SOTA performance in this task.
234 The pretrained checkpoint of the network is obtained from their official repository. Since FB-Occ
235 predicts occupancy using only single frame images, we thus train SytheOcc without cross-frame
236 attention in related experiments. For video generation, we provide experimental results in appendix.

237 **Metrics** We use Frechet Inception Distance (FID) [6] to measure the perceptual quality of generated
238 images, and use mIoU to measure the precision of occupancy prediction.

239 **Hyperparameters** We set $D = 256$, $d_{min} = 0$ and $d_{max} = 50$. The depth resolution of MPI is
240 thus higher than occupancy voxel. We train our model in 6 epochs with batch size = 8. The learning
241 rate is set at $2e^{-5}$. The training phase takes around 1 day using 8 NVIDIA A100 80G GPUs. We use
242 UniPC scheduler [42] with the classifier-free guidance (CFG) [7] that is set as 7.0. During inference,
243 we use 20 denoising steps for dataset generation.

244 **Baselines** We compare our method with prior methods in Tab. 1. ControlNet denotes we train
245 a ControlNet using an RGB semantic mask as the condition. ControlNet+depth denotes we add a
246 depth channel after the semantic mask to provide 2.5D depth information. The depth map rendered
247 by occupancy is normalized to [0-255] to accommodate the RGB value. The ControlNet+depth can
248 be regarded as a degradation of SytheOcc which is reduced to a single plane. Then we evaluate
249 MagicDrive since it is the only open-sourced method in this area. MagicDrive separately encodes
250 foreground and background using prompt and BEV layout. Furthermore, we evaluate the image
251 quality (FID [6]) of our method in Tab. 2. Compared with prior methods, we use a unified 3D
252 representation that seamlessly handles foreground and background, surpassing them by a large margin.

253 4.2 Qualitative Results

254 **High-level Control using Prompt** In Fig. 5 (c,d) and Fig. 6 (c), we demonstrate the capability
255 to employ user-defined prompts to generate images with specific weather conditions and high-level

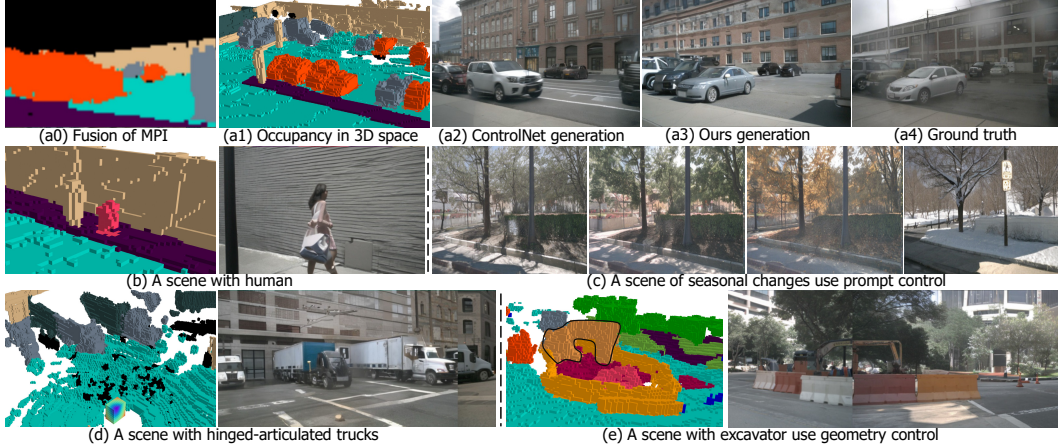


Figure 6: **Top row:** Comparison with ControlNet. We achieve a precise alignment between conditional labels and synthesized images, while ControlNet generates objects with incorrect pose due to ambiguous 2D condition. **Mid and Bottom row:** Visualizations of geometry-controlled image generation. We can faithfully generate objects with the desired topology in a specific 3D position.

256 style. Although the nuScenes dataset doesn’t contain rare weather images like snow and sandstorms,
 257 our method successfully conveys prior knowledge pretrained from stable diffusion to our scenes.
 258 Compared with visualization results in prior work like Fig. 8 of MagicDrive, our method shows better
 259 alignment with the text prompt, demonstrating the cross-domain generalization ability of our method.

260 **3D Geometric Control** Our flexible framework enables us to create novel scenes by manipulating
 261 voxels as displayed in Fig. 1 and Fig. 3. Basically, we can edit the occupied state and semantics of
 262 every voxel in our scenes for generation. We highlight that we can create a hinged-articulated truck
 263 and an excavator as shown in Fig. 6 (d,e). The generated excavator image exhibits a remarkable
 264 alignment with the input occupancy that is delineated by a black outline.

265 **Long-tailed Scene Generation** The flexibility of 3D semantic MPI has conferred significant
 266 advantages upon our approach. In the following, we create long-tail scenes that rarely occur in
 267 our real world for evaluation. In Fig. 1, we show that we manually add parallel traffic cones in
 268 front of the ego vehicle. This scene has never happened in the training dataset, but our geometric
 269 controllability provides us the capability to create such data. We then use the created scene to test
 270 autonomous driving systems such as end-to-end planner VAD [9] to validate its effectiveness. In
 271 this case, VAD successfully predicts correct waypoints with the high-level command ‘turn left’.
 272 Moreover, in appendix Sec. B, we generate long-tailed scenes with extreme weather such as snow
 273 and sandstorms, and evaluate perception model on it to examine its generalizability of rare weather.

274 **Comparison with Baselines** In Fig. 6 (a), we visualize a comparison with ControlNet. We find
 275 that ControlNet struggles to distinguish the overlapping instances in 2D-pixel space. This leads to the
 276 two parked cars being merged into a single car with incorrect pose. In contrast, our 3D semantic MPIs
 277 contain more than 2D semantic mask, but also account for complete scene geometry with occluded

Method	Condition Type	FID
BEVGen [23]	BEV map	25.54
BEVControl [34]	BEV map	24.85
DriveDreamer [26]	Box + FoV map	52.60
MagicDrive [5]	Box + BEV map	16.20
Panacea [30]	Box + FoV map	16.96
Ours	3D Semantic MPI	14.75

Table 2: Comparison of FID with previous methods on the nuScenes dataset.

MPI Encoder	Reweighting Method			Metric
design	Progressive	Depth	CBGS	mIoU
3×3	-	-	-	21.96
1×1	-	-	-	23.05
1×1	✓	-	-	23.63
1×1	✓	✓	-	24.40
1×1	✓	✓	✓	25.50

Table 3: Ablation of different designs of the MPI encoder and reweighting methods.

278 parts. Together with our proposed MPI encoder and reweighing strategy, our framework yields a
279 realistic image generation with high-quality label alignment. More comparison is provided in Sec. D.

280 4.3 Quantitative Results

281 **Recognizability, Realism and Controllability Evaluation** To evaluate whether our generated
282 images aligned with given annotations, we provide Gen experiment in Tab. 1. Using the annotation of
283 val set, we synthesize a copy of val set’s images, then use perception model trained on real training set
284 to perform evaluation. The performance will be more effective as it is close to the oracle performance.
285 We find that local method (ControlNet) perform better than global method (MagicDrive). Furthermore,
286 SytheOcc generalizes the locality for 3D conditioning to yield better performance.

287 **Data Augmentation for 3D Occupancy Prediction** Notably, we conduct experiments using our
288 synthesized dataset to enhance the real training set in Tab. 1. We first use the occupancy labels from
289 training set to create a synthetic training set. Then we modify the loading pipeline in perception model
290 to randomly sample images from real dataset or synthetic dataset and train network from scratch.
291 Therefore, our approach preserves the inherent training dynamics of the neural network by solely
292 modifying the training images, without any alteration to the number of training iterations or epochs.
293 As MagicDrive-Aug exhibits numerical overflow when training FB-Occ, which may attributed to
294 unsatisfactory recognizability, we have to omit it and only provide MagicDrive-Gen experiments.

295 As shown in Tab. 1, where SytheOcc-Aug denotes the augmentation experiments using our generated
296 dataset, shows a satisfactory improvement over the prior state of the art. We emphasize that surpassing
297 the performance of the original dataset is not the primary objective of our work; rather, it is an
298 ancillary benefit that emerges from our framework for geometry-controlled generation.

299 **Ablations** In Tab. 3, we present ablation studies across several design spaces of our model, analo-
300 gous to the Gen experiment in Tab. 1. We find that our designed MPI encoder of 1×1 conv have sig-
301 nificant improvement when compared to the conventional 3×3 conv approach. Besides, our proposed
302 three types of reweighing methods demonstrate a consistent improvement over the baseline. As a
303 result, the improved image quality and label alignment enable higher precision in downstream tasks.

304 5 Limitation and Broader Impacts

305 **Layout Generation** Our method is restricted in a conditional generation framework that should
306 have a conditional input at first. Our condition signal is from the original dataset annotation. Thus
307 most of the augmented data is generated using the same occupancy layout, or with minimal human
308 editing. Future research can incorporate the recent research [10, 17, 32, 40] that generates occupancy
309 descriptions of the scenes to synthesize images with novel occupancy layouts.

310 **Closed-loop Simulation** Given the underlying diverse and controllable image generation of our
311 method, it would be advantageous and valuable to extend our work to a broader domain such as closed-
312 loop simulation [16, 38], to enable high-fidelity autonomous systems testing. This line of work can
313 be conducted by utilizing motion conditions to generate future frames as in world model [17, 28, 36],
314 or by explicitly modeling scene graph as in the case of UniSim [20, 38] and NeuroNCAP [16].

315 **Long-tailed Scene Generation** In this paper, we only investigate a limited number of long-tailed
316 scene generation and corner case evaluations such as rare layout in Fig. 1 and extreme weather in
317 Sec. B. Future work can extend our framework to (i) Synthesize more samples for tail classes to boost
318 performance. (ii) Generate or replicate large-scale databases of corner cases [11] for robust perception.

319 6 Conclusion

320 In this paper, we propose **SytheOcc**, an innovative image generation framework that is empowered
321 with geometry-controlled capabilities using occupancy. We introduce a novel 3D representation,
322 3D semantic MPIs, to address the critical challenge of how to efficiently encode occupancy. This
323 representation not only preserves the authentic and complete 3D geometry details with semantics, but
324 also provides a spatial-align feature representation for 2D diffusion models. With this property, our
325 method enjoys photorealistic appearances and fine-grained 3D controllability, serves as a generative
326 data engine to enable a broad range of applications. Extensive experiments demonstrate that our
327 synthetic data facilitate the training for perception models on occupancy prediction, and provide
328 valuable corner case evaluation in a simulated world.

329 References

- 330 [1] Abien Fred Agarap. Deep learning using rectified linear units (relu). [arXiv preprint arXiv:1803.08375](#),
331 2018. [5](#)
- 332 [2] Holger Caesar, Varun Bankiti, Alex H. Lang, Sourabh Vora, Venice Erin Liong, Qiang Xu, Anush Krishnan,
333 Yu Pan, Giancarlo Baldan, and Oscar Beijbom. nuscenes: A multimodal dataset for autonomous driving.
334 In [CVPR](#), 2020. [7](#)
- 335 [3] Kai Chen, Enze Xie, Zhe Chen, Lanqing Hong, Zhenguo Li, and Dit-Yan Yeung. Integrating geometric
336 control into text-to-image diffusion models for high-quality detection data generation via text prompt.
337 [arXiv preprint arXiv:2306.04607](#), 2023. [3, 6](#)
- 338 [4] Jaeyoung Chung, Suyoung Lee, Hyeongjin Nam, Jaerin Lee, and Kyoung Mu Lee. Luciddreamer: Domain-
339 free generation of 3d gaussian splatting scenes. [arXiv preprint arXiv:2311.13384](#), 2023. [12](#)
- 340 [5] Ruiyuan Gao, Kai Chen, Enze Xie, Lanqing Hong, Zhenguo Li, Dit-Yan Yeung, and Qiang Xu. Magicdrive:
341 Street view generation with diverse 3d geometry control. In [ICLR](#), 2024. [1, 3, 5, 8, 14](#)
- 342 [6] Martin Heusel, Hubert Ramsauer, Thomas Unterthiner, Bernhard Nessler, and Sepp Hochreiter. Gans
343 trained by a two time-scale update rule converge to a local nash equilibrium. [NeurIPS](#), 2017. [7](#)
- 344 [7] Jonathan Ho and Tim Salimans. Classifier-free diffusion guidance. [arXiv preprint:2207.12598](#), 2022. [7](#)
- 345 [8] Lukas Höllein, Ang Cao, Andrew Owens, Justin Johnson, and Matthias Nießner. Text2room: Extracting
346 textured 3d meshes from 2d text-to-image models. In [ICCV](#), 2023. [12](#)
- 347 [9] Bo Jiang, Shaoyu Chen, Qing Xu, Bencheng Liao, Jiajie Chen, Helong Zhou, Qian Zhang, Wenyu Liu,
348 Chang Huang, and Xinggang Wang. Vad: Vectorized scene representation for efficient autonomous driving.
349 In [ICCV](#), 2023. [2, 8, 12, 13](#)
- 350 [10] Jumin Lee, Sebin Lee, Changho Jo, Woobin Im, Juhyeong Seon, and Sung-Eui Yoon. Semcity: Semantic
351 scene generation with triplane diffusion. [arXiv preprint arXiv:2403.07773](#), 2024. [9](#)
- 352 [11] Kaican Li, Kai Chen, Haoyu Wang, Lanqing Hong, Chaoqiang Ye, Jianhua Han, Yukuai Chen, Wei Zhang,
353 Chunjing Xu, Dit-Yan Yeung, et al. Coda: A real-world road corner case dataset for object detection in
354 autonomous driving. In [ECCV](#), 2022. [9](#)
- 355 [12] Leheng Li, Qing Lian, Luozhou Wang, Ningning Ma, and Ying-Cong Chen. Lift3d: Synthesize 3d training
356 data by lifting 2d gan to 3d generative radiance field. In [CVPR](#), 2023. [1, 3](#)
- 357 [13] Xiaofan Li, Yifu Zhang, and Xiaoqing Ye. Drivingdiffusion: Layout-guided multi-view driving scene
358 video generation with latent diffusion model. [arXiv preprint arXiv:2310.07771](#), 2023. [3](#)
- 359 [14] Yuheng Li, Haotian Liu, Qingyang Wu, Fangzhou Mu, Jianwei Yang, Jianfeng Gao, Chunyuan Li, and
360 Yong Jae Lee. Gligen: Open-set grounded text-to-image generation. In [CVPR](#), 2023. [2](#)
- 361 [15] Zhiqi Li, Zhiding Yu, David Austin, Mingsheng Fang, Shiyi Lan, Jan Kautz, and Jose M Alvarez.
362 Fb-occ: 3d occupancy prediction based on forward-backward view transformation. [arXiv preprint](#)
363 [arXiv:2307.01492](#), 2023. [7](#)
- 364 [16] William Ljungbergh, Adam Tonderski, Joakim Johnander, Holger Caesar, Kalle Åström, Michael Felsberg,
365 and Christoffer Petersson. Neuroncap: Photorealistic closed-loop safety testing for autonomous driving.
366 [arXiv preprint arXiv:2404.07762](#), 2024. [9](#)
- 367 [17] Jiachen Lu, Ze Huang, Jiahui Zhang, Zeyu Yang, and Li Zhang. Wovogen: World volume-aware diffusion
368 for controllable multi-camera driving scene generation. [arXiv preprint arXiv:2312.02934](#), 2023. [3, 9](#)
- 369 [18] Jianbiao Mei, Yu Yang, Mengmeng Wang, Tianxin Huang, Xuemeng Yang, and Yong Liu. Ssc-rs: Elevate
370 lidar semantic scene completion with representation separation and bev fusion. In [IROS](#), 2023. [3](#)
- 371 [19] Ben Mildenhall, Pratul P. Srinivasan, Matthew Tancik, Jonathan T. Barron, Ravi Ramamoorthi, and Ren
372 Ng. Nerf: Representing scenes as neural radiance fields for view synthesis. In [ECCV](#), 2020. [1](#)
- 373 [20] Julian Ost, Fahim Mannan, Nils Thuerey, Julian Knodt, and Felix Heide. Neural scene graphs for dynamic
374 scenes. In [CVPR](#), 2021. [9](#)
- 375 [21] Robin Rombach, Andreas Blattmann, Dominik Lorenz, Patrick Esser, and Björn Ommer. High-resolution
376 image synthesis with latent diffusion models. In [CVPR](#), 2022. [3, 7](#)
- 377 [22] Liangchen Song, Liangliang Cao, Hongyu Xu, Kai Kang, Feng Tang, Junsong Yuan, and Yang Zhao.
378 Roomdreamer: Text-driven 3d indoor scene synthesis with coherent geometry and texture. [arXiv preprint](#)
379 [arXiv:2305.11337](#), 2023. [12](#)
- 380 [23] Alexander Swerdlow, Runsheng Xu, and Bolei Zhou. Street-view image generation from a bird’s-eye view
381 layout. [IEEE RAL](#), 2024. [1, 3, 8](#)

- 382 [24] Xiaoyu Tian, Tao Jiang, Longfei Yun, Yucheng Mao, Huitong Yang, Yue Wang, Yilun Wang, and Hang
383 Zhao. Occ3d: A large-scale 3d occupancy prediction benchmark for autonomous driving. NeurIPS, 2024.
384 1, 3, 7
- 385 [25] Wenwen Tong, Chonghao Sima, Tai Wang, Li Chen, Silei Wu, Hanming Deng, Yi Gu, Lewei Lu, Ping
386 Luo, Dahua Lin, et al. Scene as occupancy. In ICCV, 2023. 3
- 387 [26] Xiaofeng Wang, Zheng Zhu, Guan Huang, Xinze Chen, and Jiwen Lu. Drivedreamer: Towards real-world-
388 driven world models for autonomous driving. arXiv preprint arXiv:2309.09777, 2023. 3, 8
- 389 [27] Xiaofeng Wang, Zheng Zhu, Wenbo Xu, Yunpeng Zhang, Yi Wei, Xu Chi, Yun Ye, Dalong Du, Jiwen
390 Lu, and Xingang Wang. Openoccupancy: A large scale benchmark for surrounding semantic occupancy
391 perception. In ICCV, 2023. 1, 3, 7
- 392 [28] Yuqi Wang, Jiawei He, Lue Fan, Hongxin Li, Yuntao Chen, and Zhaoxiang Zhang. Driving into the future:
393 Multiview visual forecasting and planning with world model for autonomous driving. arXiv preprint
394 arXiv:2311.17918, 2023. 3, 5, 9
- 395 [29] Yi Wei, Linqing Zhao, Wenzhao Zheng, Zheng Zhu, Jie Zhou, and Jiwen Lu. Surroundocc: Multi-camera
396 3d occupancy prediction for autonomous driving. In ICCV, 2023. 3
- 397 [30] Yuqing Wen, Yucheng Zhao, Yingfei Liu, Fan Jia, Yanhui Wang, Chong Luo, Chi Zhang, Tiancai Wang,
398 Xiaoyan Sun, and Xiangyu Zhang. Panacea: Panoramic and controllable video generation for autonomous
399 driving. arXiv preprint arXiv:2311.16813, 2023. 1, 3, 5, 8
- 400 [31] Jay Zhangjie Wu, Yixiao Ge, Xintao Wang, Stan Weixian Lei, Yuchao Gu, Yufei Shi, Wynne Hsu, Ying
401 Shan, Xiaohu Qie, and Mike Zheng Shou. Tune-a-video: One-shot tuning of image diffusion models for
402 text-to-video generation. In ICCV, 2023. 5, 14
- 403 [32] Zhennan Wu, Yang Li, Han Yan, Taizhang Shang, Weixuan Sun, Senbo Wang, Ruikai Cui, Weizhe Liu,
404 Hiroyuki Sato, Hongdong Li, et al. Blockfusion: Expandable 3d scene generation using latent tri-plane
405 extrapolation. arXiv preprint arXiv:2401.17053, 2024. 9
- 406 [33] Xu Yan, Jiantao Gao, Jie Li, Ruimao Zhang, Zhen Li, Rui Huang, and Shuguang Cui. Sparse single sweep
407 lidar point cloud segmentation via learning contextual shape priors from scene completion. In AAAI, 2021.
408 3
- 409 [34] Kairui Yang, Enhui Ma, Jibin Peng, Qing Guo, Di Lin, and Kaicheng Yu. Bevcontrol: Accurately
410 controlling street-view elements with multi-perspective consistency via bev sketch layout. arXiv preprint
411 arXiv:2308.01661, 2023. 3, 8
- 412 [35] Ling Yang, Zhilong Zhang, Yang Song, Shenda Hong, Runsheng Xu, Yue Zhao, Wentao Zhang, Bin Cui,
413 and Ming-Hsuan Yang. Diffusion models: A comprehensive survey of methods and applications. ACM
414 Computing Surveys, 2023. 3
- 415 [36] Mengjiao Yang, Yilun Du, Kamyar Ghasemipour, Jonathan Tompson, Dale Schuurmans, and Pieter Abbeel.
416 Learning interactive real-world simulators. arXiv preprint arXiv:2310.06114, 2023. 9
- 417 [37] Yuanbo Yang, Yifei Yang, Hanlei Guo, Rong Xiong, Yue Wang, and Yiyi Liao. Urbangiraffe: Representing
418 urban scenes as compositional generative neural feature fields. In ICCV, 2023. 3
- 419 [38] Ze Yang, Yun Chen, Jingkang Wang, Sivabalan Manivasagam, Wei-Chiu Ma, Anqi Joyce Yang, and Raquel
420 Urtasun. Unisim: A neural closed-loop sensor simulator. In CVPR, 2023. 9
- 421 [39] Hong-Xing Yu, Haoyi Duan, Junhwa Hur, Kyle Sargent, Michael Rubinstein, William T Freeman, Forrester
422 Cole, Deqing Sun, Noah Snavely, Jiajun Wu, et al. Wonderjourney: Going from anywhere to everywhere.
423 arXiv preprint arXiv:2312.03884, 2023. 12
- 424 [40] Junge Zhang, Qihang Zhang, Li Zhang, Ramana Rao Kompella, Gaowen Liu, and Bolei Zhou. Urban
425 scene diffusion through semantic occupancy map. arXiv preprint arXiv:2403.11697, 2024. 9
- 426 [41] Lvmin Zhang, Anyi Rao, and Maneesh Agrawala. Adding conditional control to text-to-image diffusion
427 models. In ICCV, 2023. 2, 3, 5
- 428 [42] Wenliang Zhao, Lujia Bai, Yongming Rao, Jie Zhou, and Jiwen Lu. Unipc: A unified predictor-corrector
429 framework for fast sampling of diffusion models. NeurIPS, 2023. 7
- 430 [43] Tinghui Zhou, Richard Tucker, John Flynn, Graham Fyffe, and Noah Snavely. Stereo magnification:
431 Learning view synthesis using multiplane images. arXiv preprint arXiv:1805.09817, 2018. 2, 4
- 432 [44] Benjin Zhu, Zhengkai Jiang, Xiangxin Zhou, Zeming Li, and Gang Yu. Class-balanced grouping and
433 sampling for point cloud 3d object detection. arXiv preprint arXiv:1908.09492, 2019. 6

Appendix

435 In the appendix, we provide the following content:

Sec. A : Statement of Geometric Control.	Sec. E : Results of Video Generation.
Sec. B : Long-Tailed Scene Evaluation.	Sec. F : Generalize to New Cameras.
Sec. C : Ablation of plane number in MPIs.	Sec. G : Impact of Amount of Augment Data.
Sec. D : Additional Qualitative Comparison.	Sec. H : Visualization of Failure Cases.

436 **A Statement of Geometric Control**

437 In our paper, we refer the geometric controllable generation as using a voxel grid in 3D space to
 438 control the image generation. Although the voxel is a quantized representation of the 3D world,
 439 when the resolution goes larger, it can already faithfully represent the geometry detail of scenes.
 440 Currently, we are limited by the precision of ground truth labels. The $0.2m$ occupancy grid is a tensor
 441 of $500 \times 500 \times 40$ that cover a space in x-axis spanning $[-50m, 50m]$, y-axis spanning $[-50m, 50m]$,
 442 z-axis spanning $[-5m, 3m]$. In the future, we plan to explore a higher resolution of geometric control
 443 to refine our generation.

444 Except for occupancy, several other 3D representations can be expressed by 3D semantic MPI,
 445 such as mesh, dense point clouds, and even 3D boxes or HD maps. The underlying mechanism is
 446 to cast several slices of multi-plane images at different depths to retrieve geometric information.
 447 Thus, our 3D semantic MPI can be regarded as a general 3D conditioning representation to benefit
 448 a wide spectrum of practical systems. These encompass but are not limited to 3D generation such
 449 as text2room [8], RoomDreamer [22], WonderJourney [39], and LucidDreamer [4], each of which
 450 stands to benefit from the rich geometric context provided by our approach.

451 **B Long-Tailed Scene Evaluation**

452 In this section, we explore to use SytheOcc to create long-tailed scenes for downstream evaluation.
 453 This also stands for evaluating our model using several corner cases. Similar to the SytheOcc-Gen
 454 experiment in Tab. 1, we generate a synthetic validation set but use prompts control to manipulate
 455 weather patterns or the intensity of illumination.

456 As depicted in Fig. 7. We create a variety of weather conditions including sandstorms, snow, foggy,
 457 rainy, day night, and day time. The motivation behind the creation of these scenes lies in their extreme
 458 rarity compared to the ordinary scenes we have captured. The generation of such data is of significant
 459 value, as it aids in addressing the long-tailed distribution of scenes, thereby enriching the diversity of
 460 our dataset. More visualization is provided in Fig. 13 to Fig. 14.

461 In Tab. 4, we observe that all kinds of extreme weather lead to a degradation in performance. This
 462 observation underscores the limitations of the perception model in terms of its generalizability to
 463 infrequent weather scenarios. Among them, we find that foggy, rainy, and day night exert the most
 464 severe impact, as they contribute to a large reduction in visibility as shown in Fig. 7. To improve the
 465 generalizability to handle various weather conditions, future work can leverage our generated data to
 466 cover the long-tailed scenes, or use adversarial search to find severe scenes based on our framework.

Scenes	Sandstorm	Snow	Foggy	Rainy	Day night	Day time (raw data)
FB-Occ mIOU	22.88	18.25	10.29	9.71	9.95	25.50

Table 4: Experiments of downstream evaluation on long-tailed scenes with extreme weather.

467 Furthermore, we perform long-tailed scene evaluation in Fig. 8. We display the failure of the
 468 downstream model VAD [9] in our synthetic long-tailed scene. In this case, we simulate a foggy
 469 environment that the dense fog obscures the majority of the ego view. Our experiment reveals that
 470 due to the lack of training images of foggy scenes, VAD erroneously predicts waypoints that would
 471 result in a collision with the bus. This experiment elucidates the boundaries and failure cases of the
 472 VAD model [9]. It exposes the limitations of the system under certain conditions, thereby providing
 473 insights into scenarios where the model’s performance may be compromised.

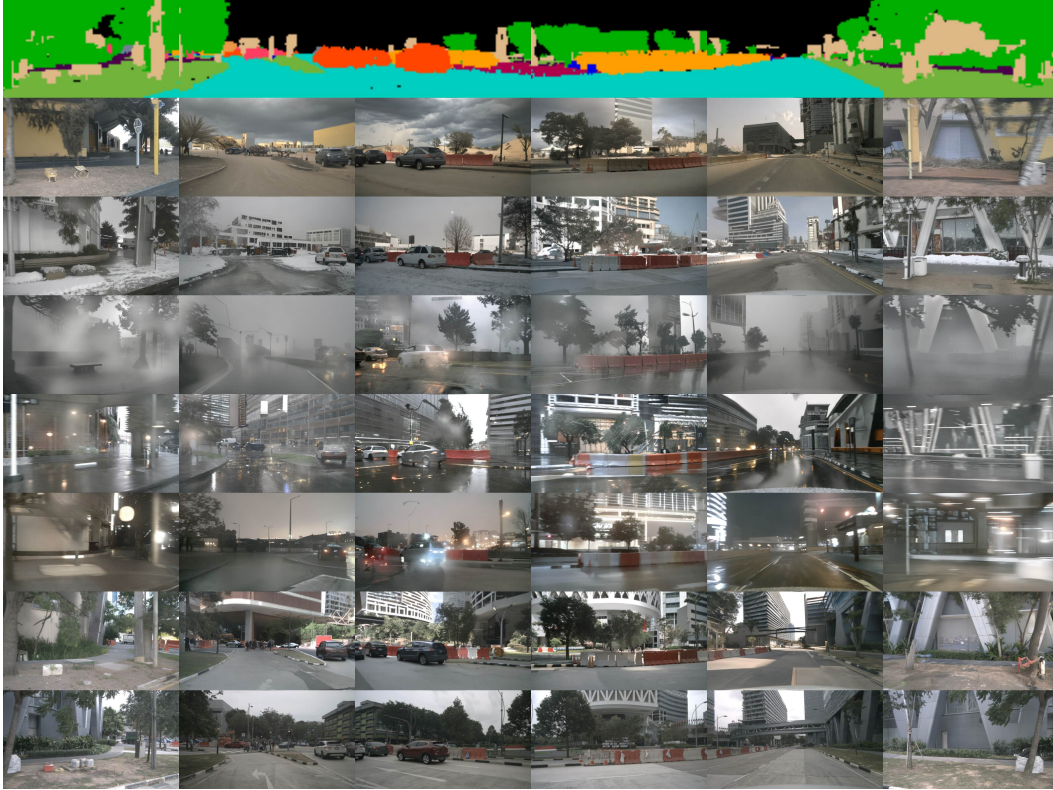


Figure 7: From top to bottom, we display images of fusion of 3D semantic MPI, synthesized images of sandstorm, snow, foggy, rainy, day night, day time, and ground truth.

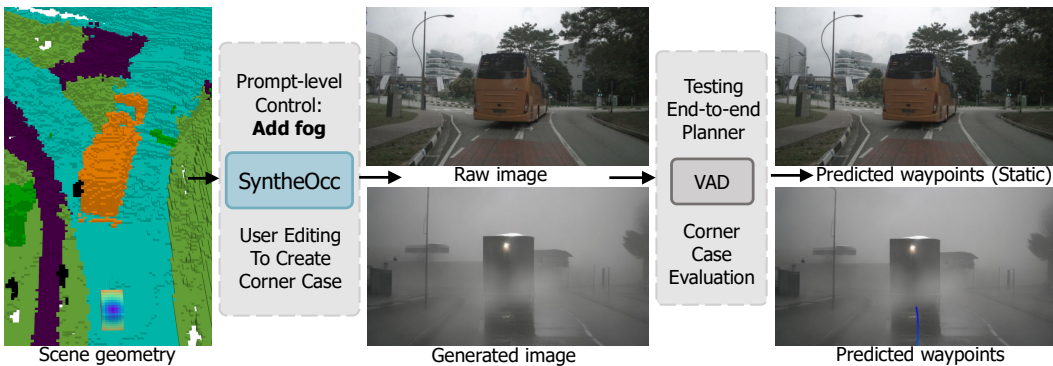


Figure 8: Use **SyntheOcc** to create long-tailed scenes for testing. **Top**: In the ordinary scene of a bus placed in front of the ego vehicle, the end-to-end planner VAD [9] predicts future waypoints without movement, thus not plotted in the image. **Bottom**: By harnessing the prompt-level control in our framework, we simulate a scene with the same layout but filled with fog. VAD predicts wrong waypoints that will collide with the bus.

474 C Ablation of plane number of MPIs

475 In our proposed 3D semantic MPIs, the number of planes is a hyperparameter that affects the precision
 476 of 3D representation. The plane number can be regarded as the 3D resolution in depth axis. The
 477 larger the plane number, the MPI will contain more details. We find that an increase in the number of
 478 planes is associated with improved accuracy in downstream tasks. This finding denotes that more
 479 condition information leads to better downstream task performance.



Figure 9: Comparison with baselines.

Number of Planes	96	128	256
FB-Occ mIOU	23.36	24.28	25.50

Table 5: Ablation of the number of multi-plane images.

480 D Qualitative Comparison with Baselines and SOTA

481 In Fig. 9, we conduct a qualitative comparison of our method against MagicDrive, ControlNet, and
 482 ControlNet+depth. We find that all the methods display a satisfactory image quality, as they build upon
 483 the foundation of the stable diffusion model. The generation of MagicDrive fails to synthesize barriers
 484 as shown in the bottom row. ControlNet struggles to generate objects with the correct pose solely
 485 from only 2D conditions as shown in the second row. ControlNet+depth, a degradation of our method,
 486 an enhancement over ControlNet in terms of alignment, nevertheless suffers from a loss of finer detail
 487 in scenes with heavy occlusion, as shown in the human of the third row. Our method, in contrast, aims
 488 to address these challenges and provide a more nuanced and accurate generation of complex scenes.

489 E Extend to Video Generation

490 As described in the main paper Sec. 3.4, we further extend the cross-view attention to cross-frame
 491 attention to perform video generation. Our generation results are Fig. 11, Fig. 12 and Fig. 16.
 492 Our implementation is adopted from MagicDrive [5] which is similar to Tune-a-video [31]. The
 493 formulation of cross-frame attention is:

$$\text{Attention}(Q, K, V) = \text{softmax}\left(\frac{QK^T}{\sqrt{d}}\right) \cdot V, \quad (8)$$

$$h_{out} = h_{in} + \sum_{i \in \{f, h\}} \text{Attention}(Q_{in}, K_i, V_i), \quad (9)$$

494 where f , and h are the camera view of future and history frames. Q_{in} and h_{in} denotes the query and
 495 the hidden state of input view. We train our model in a two-stage pipeline. We first train the MPI
 496 encoder and cross-view attention in a multi-view image generation setting. Then we train cross-frame
 497 attention and freeze other components in a video generation setting.

498 In practice, we use the keyframe annotation of the nuScenes dataset to train our video model. We start
 499 with our pretrained MPI encoder and cross-view attention and only train our cross-frame attention
 500 while keeping others frozen. We employ a sequence of 7 frames as a batch, resulting in a batch size
 501 of 42 images for the training process.

502 Given that our primary contribution does not lie in video generation, this experiment serves as a
 503 proof of concept, demonstrating the potential of our framework. Future research may extend our
 504 methodology to facilitate the generation of longer video sequences, thereby expanding the scope and
 505 applicability of our framework.

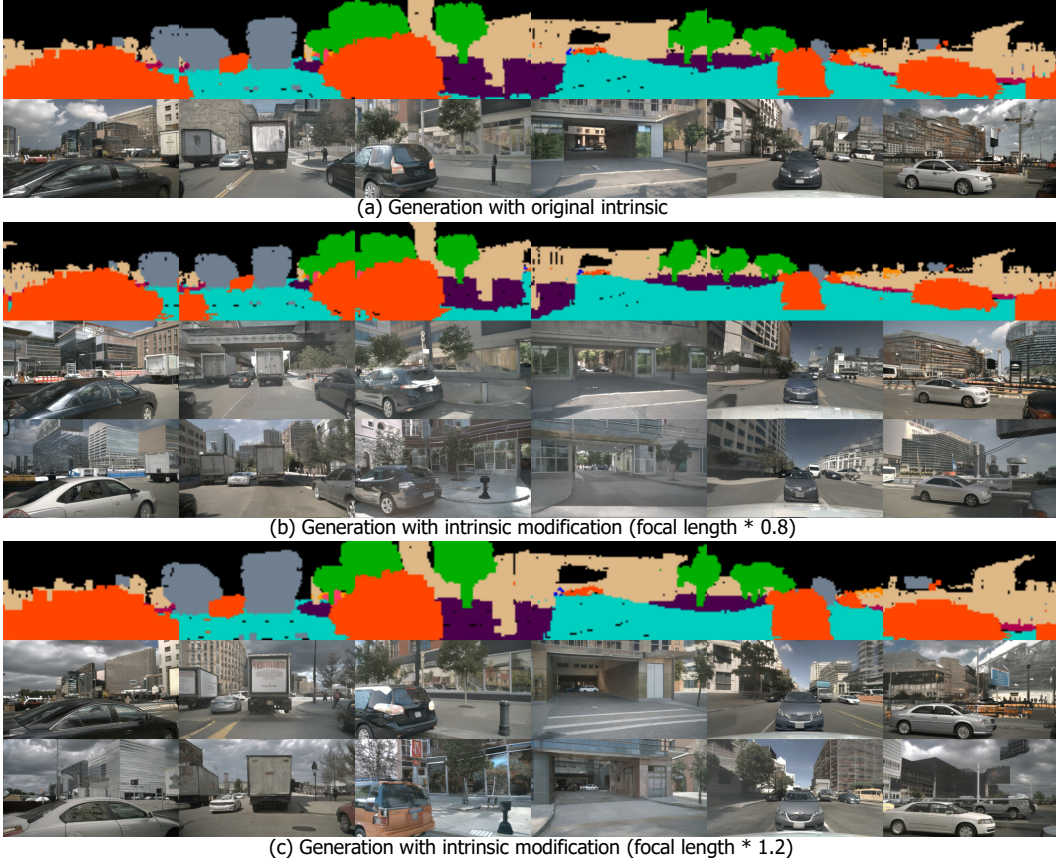


Figure 10: We demonstrate the generalizability of SytheOcc to new camera intrinsic. We multiply factors to the focal length while keeping the resolution the same. In (b,c), focal length $\times 0.8$ denotes a camera with a larger field of view similar to zoom out, focal length $\times 1.2$ denotes a camera with a smaller field of view similar to zoom in.

506 F Generalize to New Cameras

507 In this section, we investigate the adaptability of our method to a new set of cameras with different
 508 intrinsic. Given that our training set has a fixed camera intrinsic and extrinsic, generalizing to novel
 509 cameras indicates that our approach possesses robust generalization capabilities. As shown in Fig. 10,
 510 benefiting from our local type of condition, SytheOcc generates images that faithfully align with
 511 the new intrinsic, proving that SytheOcc do not over-fit certain parameters. Regarding extrinsic
 512 parameters, we can cast our MPI at the desirable locations to retrieve geometric information, thus
 513 inherently ensuring generalizability without doubt.

514 G The Influence of the Amount of Augmented Data

515 As SytheOcc is capable of generating an infinite number of synthetic data, we investigate the influence
 516 of the amount of augmented data on downstream tasks in Tab. 6. We find that when our augmented
 517 data is expanded from one-fold to two-fold of the training dataset, the performance of perception
 518 model slightly decreases. This may indicate the generated data has an optimal ratio for downstream
 519 tasks. Due to limited computational resources, we only experiment with a limited amount of ratio.
 520 Future work can conduct more thorough experiments to find a universal theorem.

Amount of Augmented Data	0 (no augmentation)	1	2
FB-Occ mIOU	39.3	40.3	40.1

Table 6: Ablation of the amount of augmented data.



Figure 11: Video generation results. In the temporal progression, the distant buildings maintain a high degree of consistency, and objects retain their identical shapes and textures across different views and frames.



Figure 12: Video generation results of large dynamics scenes. The white car comes across different views and frames depicting consistent shapes with only a slight appearance change.



Figure 13: From top to bottom, we display images of fusion of 3D semantic MPI, synthesized images of sandstorm, snow, foggy, rainy, day night, day time, and ground truth.

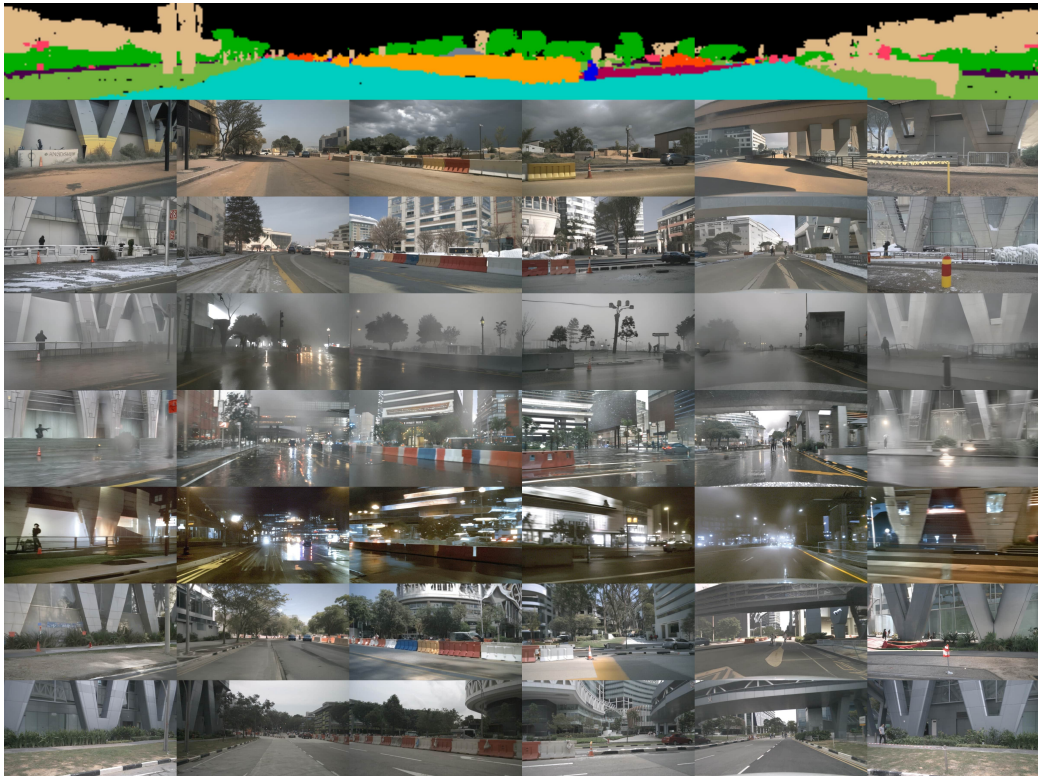


Figure 14: Weather variation. Same structure with Fig. 13.



Figure 15: Out of distribution generation. We use prompts to control the high-level appearance of images with specific styles. From top to bottom, we display (1) fusion of 3D semantic MPI. (2) Sunny day. (3) Science fiction style. (4) 8-bit pixel art style. (5) Snowfall. (6) Minecraft style. (7) Pokémon style. (8) Diablo style. (9) Ghibli style. (10) Metropolis style. (11) Gotham style. (12) Ground truth.

521 **H Failure Cases**

522 We display several failure cases of our method. In Fig. 16, we show a crowd scenes. In this scenario,
523 the excessive number of pedestrians presents a challenge to the cross-view attention and cross-frame
524 attention modules. We find our method incapable of discerning individual entities with clarity. Future
525 research can improve the model capacity or enrich high-quality data to mitigate this problem.



Figure 16: Failure case of video generation results. Our cross-frame attention module is challenging to distinguish a crowd of people across different views and frames.

526 **NeurIPS Paper Checklist**

527 The checklist is designed to encourage best practices for responsible machine learning research,
528 addressing issues of reproducibility, transparency, research ethics, and societal impact. Do not remove
529 the checklist: **The papers not including the checklist will be desk rejected.** The checklist should
530 follow the references and follow the (optional) supplemental material. The checklist does NOT count
531 towards the page limit.

532 Please read the checklist guidelines carefully for information on how to answer these questions. For
533 each question in the checklist:

- 534 • You should answer [Yes], [No], or [NA].
- 535 • [NA] means either that the question is Not Applicable for that particular paper or the
536 relevant information is Not Available.
- 537 • Please provide a short (1–2 sentence) justification right after your answer (even for NA).

538 **The checklist answers are an integral part of your paper submission.** They are visible to the
539 reviewers, area chairs, senior area chairs, and ethics reviewers. You will be asked to also include it
540 (after eventual revisions) with the final version of your paper, and its final version will be published
541 with the paper.

542 The reviewers of your paper will be asked to use the checklist as one of the factors in their evaluation.
543 While "[Yes]" is generally preferable to "[No]", it is perfectly acceptable to answer "[No]" provided a
544 proper justification is given (e.g., "error bars are not reported because it would be too computationally
545 expensive" or "we were unable to find the license for the dataset we used"). In general, answering
546 "[No]" or "[NA]" is not grounds for rejection. While the questions are phrased in a binary way, we
547 acknowledge that the true answer is often more nuanced, so please just use your best judgment and
548 write a justification to elaborate. All supporting evidence can appear either in the main paper or the
549 supplemental material, provided in appendix. If you answer [Yes] to a question, in the justification
550 please point to the section(s) where related material for the question can be found.

551 **IMPORTANT, please:**

- 552 • **Delete this instruction block, but keep the section heading “NeurIPS paper checklist”.**
- 553 • **Keep the checklist subsection headings, questions/answers and guidelines below.**
- 554 • **Do not modify the questions and only use the provided macros for your answers.**

555 **1. Claims**

556 Question: Do the main claims made in the abstract and introduction accurately reflect the
557 paper’s contributions and scope?

558 Answer: [Yes]

559 Justification: Please find this part in Sec. 3.

560 Guidelines:

- 561 • The answer NA means that the abstract and introduction do not include the claims
562 made in the paper.
- 563 • The abstract and/or introduction should clearly state the claims made, including the
564 contributions made in the paper and important assumptions and limitations. A No or
565 NA answer to this question will not be perceived well by the reviewers.
- 566 • The claims made should match theoretical and experimental results, and reflect how
567 much the results can be expected to generalize to other settings.
- 568 • It is fine to include aspirational goals as motivation as long as it is clear that these goals
569 are not attained by the paper.

570 **2. Limitations**

571 Question: Does the paper discuss the limitations of the work performed by the authors?

572 Answer: [Yes]

573 Justification: Please find this part in Sec. 5.

574
575
576
577
578
579
580
581
582
583
584
585
586
587
588
589
590
591
592
593
594
595
596
597
598
599
600
601
602
603
604
605
606
607
608
609
610
611
612
613
614
615
616
617
618
619
620
621
622
623
624

Guidelines:

- The answer NA means that the paper has no limitation while the answer No means that the paper has limitations, but those are not discussed in the paper.
- The authors are encouraged to create a separate "Limitations" section in their paper.
- The paper should point out any strong assumptions and how robust the results are to violations of these assumptions (e.g., independence assumptions, noiseless settings, model well-specification, asymptotic approximations only holding locally). The authors should reflect on how these assumptions might be violated in practice and what the implications would be.
- The authors should reflect on the scope of the claims made, e.g., if the approach was only tested on a few datasets or with a few runs. In general, empirical results often depend on implicit assumptions, which should be articulated.
- The authors should reflect on the factors that influence the performance of the approach. For example, a facial recognition algorithm may perform poorly when image resolution is low or images are taken in low lighting. Or a speech-to-text system might not be used reliably to provide closed captions for online lectures because it fails to handle technical jargon.
- The authors should discuss the computational efficiency of the proposed algorithms and how they scale with dataset size.
- If applicable, the authors should discuss possible limitations of their approach to address problems of privacy and fairness.
- While the authors might fear that complete honesty about limitations might be used by reviewers as grounds for rejection, a worse outcome might be that reviewers discover limitations that aren't acknowledged in the paper. The authors should use their best judgment and recognize that individual actions in favor of transparency play an important role in developing norms that preserve the integrity of the community. Reviewers will be specifically instructed to not penalize honesty concerning limitations.

3. Theory Assumptions and Proofs

Question: For each theoretical result, does the paper provide the full set of assumptions and a complete (and correct) proof?

Answer: [NA]

Justification: The paper does not include theoretical results.

Guidelines: Do not have theoretical results.

- The answer NA means that the paper does not include theoretical results.
- All the theorems, formulas, and proofs in the paper should be numbered and cross-referenced.
- All assumptions should be clearly stated or referenced in the statement of any theorems.
- The proofs can either appear in the main paper or the supplemental material, but if they appear in the supplemental material, the authors are encouraged to provide a short proof sketch to provide intuition.
- Inversely, any informal proof provided in the core of the paper should be complemented by formal proofs provided in appendix or supplemental material.
- Theorems and Lemmas that the proof relies upon should be properly referenced.

4. Experimental Result Reproducibility

Question: Does the paper fully disclose all the information needed to reproduce the main experimental results of the paper to the extent that it affects the main claims and/or conclusions of the paper (regardless of whether the code and data are provided or not)?

Answer: [Yes]

Justification: Please find this part in Sec. 4.

Guidelines:

- The answer NA means that the paper does not include experiments.

- 625 • If the paper includes experiments, a No answer to this question will not be perceived
626 well by the reviewers: Making the paper reproducible is important, regardless of
627 whether the code and data are provided or not.
- 628 • If the contribution is a dataset and/or model, the authors should describe the steps taken
629 to make their results reproducible or verifiable.
- 630 • Depending on the contribution, reproducibility can be accomplished in various ways.
631 For example, if the contribution is a novel architecture, describing the architecture fully
632 might suffice, or if the contribution is a specific model and empirical evaluation, it may
633 be necessary to either make it possible for others to replicate the model with the same
634 dataset, or provide access to the model. In general, releasing code and data is often
635 one good way to accomplish this, but reproducibility can also be provided via detailed
636 instructions for how to replicate the results, access to a hosted model (e.g., in the case
637 of a large language model), releasing of a model checkpoint, or other means that are
638 appropriate to the research performed.
- 639 • While NeurIPS does not require releasing code, the conference does require all submis-
640 sions to provide some reasonable avenue for reproducibility, which may depend on the
641 nature of the contribution. For example
 - 642 (a) If the contribution is primarily a new algorithm, the paper should make it clear how
643 to reproduce that algorithm.
 - 644 (b) If the contribution is primarily a new model architecture, the paper should describe
645 the architecture clearly and fully.
 - 646 (c) If the contribution is a new model (e.g., a large language model), then there should
647 either be a way to access this model for reproducing the results or a way to reproduce
648 the model (e.g., with an open-source dataset or instructions for how to construct
649 the dataset).
 - 650 (d) We recognize that reproducibility may be tricky in some cases, in which case
651 authors are welcome to describe the particular way they provide for reproducibility.
652 In the case of closed-source models, it may be that access to the model is limited in
653 some way (e.g., to registered users), but it should be possible for other researchers
654 to have some path to reproducing or verifying the results.

655 5. Open access to data and code

656 Question: Does the paper provide open access to the data and code, with sufficient instruc-
657 tions to faithfully reproduce the main experimental results, as described in supplemental
658 material?

659 Answer: [Yes]

660 Justification: Please find this part in Sec. 4.

661 Guidelines:

- 662 • The answer NA means that paper does not include experiments requiring code.
- 663 • Please see the NeurIPS code and data submission guidelines ([https://nips.cc/
664 public/guides/CodeSubmissionPolicy](https://nips.cc/public/guides/CodeSubmissionPolicy)) for more details.
- 665 • While we encourage the release of code and data, we understand that this might not be
666 possible, so “No” is an acceptable answer. Papers cannot be rejected simply for not
667 including code, unless this is central to the contribution (e.g., for a new open-source
668 benchmark).
- 669 • The instructions should contain the exact command and environment needed to run to
670 reproduce the results. See the NeurIPS code and data submission guidelines ([https:
671 //nips.cc/public/guides/CodeSubmissionPolicy](https://nips.cc/public/guides/CodeSubmissionPolicy)) for more details.
- 672 • The authors should provide instructions on data access and preparation, including how
673 to access the raw data, preprocessed data, intermediate data, and generated data, etc.
- 674 • The authors should provide scripts to reproduce all experimental results for the new
675 proposed method and baselines. If only a subset of experiments are reproducible, they
676 should state which ones are omitted from the script and why.
- 677 • At submission time, to preserve anonymity, the authors should release anonymized
678 versions (if applicable).

679 • Providing as much information as possible in supplemental material (appended to the
680 paper) is recommended, but including URLs to data and code is permitted.

681 6. Experimental Setting/Details

682 Question: Does the paper specify all the training and test details (e.g., data splits, hyperpa-
683 rameters, how they were chosen, type of optimizer, etc.) necessary to understand the results?

684 Answer: [Yes]

685 Justification: Please find this part in Sec. 4.

686 Guidelines:

- 687 • The answer NA means that the paper does not include experiments.
- 688 • The experimental setting should be presented in the core of the paper to a level of detail
689 that is necessary to appreciate the results and make sense of them.
- 690 • The full details can be provided either with the code, in appendix, or as supplemental
691 material.

692 7. Experiment Statistical Significance

693 Question: Does the paper report error bars suitably and correctly defined or other appropriate
694 information about the statistical significance of the experiments?

695 Answer: [Yes]

696 Justification: Please find this part in Sec. 4.

697 Guidelines:

- 698 • The answer NA means that the paper does not include experiments.
- 699 • The authors should answer "Yes" if the results are accompanied by error bars, confi-
700 dence intervals, or statistical significance tests, at least for the experiments that support
701 the main claims of the paper.
- 702 • The factors of variability that the error bars are capturing should be clearly stated (for
703 example, train/test split, initialization, random drawing of some parameter, or overall
704 run with given experimental conditions).
- 705 • The method for calculating the error bars should be explained (closed form formula,
706 call to a library function, bootstrap, etc.)
- 707 • The assumptions made should be given (e.g., Normally distributed errors).
- 708 • It should be clear whether the error bar is the standard deviation or the standard error
709 of the mean.
- 710 • It is OK to report 1-sigma error bars, but one should state it. The authors should
711 preferably report a 2-sigma error bar than state that they have a 96% CI, if the hypothesis
712 of Normality of errors is not verified.
- 713 • For asymmetric distributions, the authors should be careful not to show in tables or
714 figures symmetric error bars that would yield results that are out of range (e.g. negative
715 error rates).
- 716 • If error bars are reported in tables or plots, The authors should explain in the text how
717 they were calculated and reference the corresponding figures or tables in the text.

718 8. Experiments Compute Resources

719 Question: For each experiment, does the paper provide sufficient information on the com-
720 puter resources (type of compute workers, memory, time of execution) needed to reproduce
721 the experiments?

722 Answer: [Yes]

723 Justification: Please find this part in Sec. 4.

724 Guidelines:

- 725 • The answer NA means that the paper does not include experiments.
- 726 • The paper should indicate the type of compute workers CPU or GPU, internal cluster,
727 or cloud provider, including relevant memory and storage.
- 728 • The paper should provide the amount of compute required for each of the individual
729 experimental runs as well as estimate the total compute.

- 730 • The paper should disclose whether the full research project required more compute
731 than the experiments reported in the paper (e.g., preliminary or failed experiments that
732 didn't make it into the paper).

733 9. Code Of Ethics

734 Question: Does the research conducted in the paper conform, in every respect, with the
735 NeurIPS Code of Ethics <https://neurips.cc/public/EthicsGuidelines?>

736 Answer: [Yes]

737 Justification: It should be fine.

738 Guidelines:

- 739 • The answer NA means that the authors have not reviewed the NeurIPS Code of Ethics.
- 740 • If the authors answer No, they should explain the special circumstances that require a
741 deviation from the Code of Ethics.
- 742 • The authors should make sure to preserve anonymity (e.g., if there is a special consid-
743 eration due to laws or regulations in their jurisdiction).

744 10. Broader Impacts

745 Question: Does the paper discuss both potential positive societal impacts and negative
746 societal impacts of the work performed?

747 Answer: [Yes]

748 Justification: Please find this part in Sec. 5.

749 Guidelines:

- 750 • The answer NA means that there is no societal impact of the work performed.
- 751 • If the authors answer NA or No, they should explain why their work has no societal
752 impact or why the paper does not address societal impact.
- 753 • Examples of negative societal impacts include potential malicious or unintended uses
754 (e.g., disinformation, generating fake profiles, surveillance), fairness considerations
755 (e.g., deployment of technologies that could make decisions that unfairly impact specific
756 groups), privacy considerations, and security considerations.
- 757 • The conference expects that many papers will be foundational research and not tied
758 to particular applications, let alone deployments. However, if there is a direct path to
759 any negative applications, the authors should point it out. For example, it is legitimate
760 to point out that an improvement in the quality of generative models could be used to
761 generate deepfakes for disinformation. On the other hand, it is not needed to point out
762 that a generic algorithm for optimizing neural networks could enable people to train
763 models that generate Deepfakes faster.
- 764 • The authors should consider possible harms that could arise when the technology is
765 being used as intended and functioning correctly, harms that could arise when the
766 technology is being used as intended but gives incorrect results, and harms following
767 from (intentional or unintentional) misuse of the technology.
- 768 • If there are negative societal impacts, the authors could also discuss possible mitigation
769 strategies (e.g., gated release of models, providing defenses in addition to attacks,
770 mechanisms for monitoring misuse, mechanisms to monitor how a system learns from
771 feedback over time, improving the efficiency and accessibility of ML).

772 11. Safeguards

773 Question: Does the paper describe safeguards that have been put in place for responsible
774 release of data or models that have a high risk for misuse (e.g., pretrained language models,
775 image generators, or scraped datasets)?

776 Answer: [NA]

777 Justification: Our paper poses no such risks.

778 Guidelines:

- 779 • The answer NA means that the paper poses no such risks.

- 780
- 781
- 782
- 783
- 784
- 785
- 786
- 787
- 788
- Released models that have a high risk for misuse or dual-use should be released with necessary safeguards to allow for controlled use of the model, for example by requiring that users adhere to usage guidelines or restrictions to access the model or implementing safety filters.
 - Datasets that have been scraped from the Internet could pose safety risks. The authors should describe how they avoided releasing unsafe images.
 - We recognize that providing effective safeguards is challenging, and many papers do not require this, but we encourage authors to take this into account and make a best faith effort.

789 12. Licenses for existing assets

790 Question: Are the creators or original owners of assets (e.g., code, data, models), used in
791 the paper, properly credited and are the license and terms of use explicitly mentioned and
792 properly respected?

793 Answer: [Yes]

794 Justification: Please find this part in Sec. 4.

795 Guidelines:

- 796
- 797
- 798
- 799
- 800
- 801
- 802
- 803
- 804
- 805
- 806
- 807
- 808
- 809
- 810
- The answer NA means that the paper does not use existing assets.
 - The authors should cite the original paper that produced the code package or dataset.
 - The authors should state which version of the asset is used and, if possible, include a URL.
 - The name of the license (e.g., CC-BY 4.0) should be included for each asset.
 - For scraped data from a particular source (e.g., website), the copyright and terms of service of that source should be provided.
 - If assets are released, the license, copyright information, and terms of use in the package should be provided. For popular datasets, paperswithcode.com/datasets has curated licenses for some datasets. Their licensing guide can help determine the license of a dataset.
 - For existing datasets that are re-packaged, both the original license and the license of the derived asset (if it has changed) should be provided.
 - If this information is not available online, the authors are encouraged to reach out to the asset's creators.

811 13. New Assets

812 Question: Are new assets introduced in the paper well documented and is the documentation
813 provided alongside the assets?

814 Answer: [NA]

815 Justification: Our paper does not release new assets.

816 Guidelines:

- 817
- 818
- 819
- 820
- 821
- 822
- 823
- 824
- The answer NA means that the paper does not release new assets.
 - Researchers should communicate the details of the dataset/code/model as part of their submissions via structured templates. This includes details about training, license, limitations, etc.
 - The paper should discuss whether and how consent was obtained from people whose asset is used.
 - At submission time, remember to anonymize your assets (if applicable). You can either create an anonymized URL or include an anonymized zip file.

825 14. Crowdsourcing and Research with Human Subjects

826 Question: For crowdsourcing experiments and research with human subjects, does the paper
827 include the full text of instructions given to participants and screenshots, if applicable, as
828 well as details about compensation (if any)?

829 Answer: [NA]

830 Justification: Our paper does not involve crowdsourcing nor research with human subjects.

831
832
833
834
835
836
837
838
839
840
841
842
843
844
845
846
847
848
849
850
851
852
853
854
855
856
857
858

Guidelines:

- The answer NA means that the paper does not involve crowdsourcing nor research with human subjects.
- Including this information in the supplemental material is fine, but if the main contribution of the paper involves human subjects, then as much detail as possible should be included in the main paper.
- According to the NeurIPS Code of Ethics, workers involved in data collection, curation, or other labor should be paid at least the minimum wage in the country of the data collector.

15. Institutional Review Board (IRB) Approvals or Equivalent for Research with Human Subjects

Question: Does the paper describe potential risks incurred by study participants, whether such risks were disclosed to the subjects, and whether Institutional Review Board (IRB) approvals (or an equivalent approval/review based on the requirements of your country or institution) were obtained?

Answer: [NA]

Justification: Our paper does not involve crowdsourcing nor research with human subjects.

Guidelines:

- The answer NA means that the paper does not involve crowdsourcing nor research with human subjects.
- Depending on the country in which research is conducted, IRB approval (or equivalent) may be required for any human subjects research. If you obtained IRB approval, you should clearly state this in the paper.
- We recognize that the procedures for this may vary significantly between institutions and locations, and we expect authors to adhere to the NeurIPS Code of Ethics and the guidelines for their institution.
- For initial submissions, do not include any information that would break anonymity (if applicable), such as the institution conducting the review.